

Analytical Methods

Advancing Methods and Applications

www.rsc.org/methods

Volume 3 | Number 1 | January 2011 | Pages 1–228



ISSN 1759-9660

RSC Publishing

PAPER

Biró *et al.*

Color based discrimination of chitin–air nanocomposites in butterfly scales and their role in conspecific recognition



1759-9660 (2011) 3:1;1-8

Color based discrimination of chitin–air nanocomposites in butterfly scales and their role in conspecific recognition

Gábor Piszter,^a Krisztián Kertész,^a Zofia Vértesy,^a Zsolt Bálint^b and László Péter Biró^{*a}

Received 28th June 2010, Accepted 21st October 2010

DOI: 10.1039/c0ay00410c

The self-assembled photonic nanoarchitectures occurring in the wing scales of the blue colored males of nine Lycaenid butterfly species, living in the same habitat, were investigated by reflectance measurements followed by automated data processing. The spectral signatures of the nine species analyzed using an artificial neural network software show that despite the fact that all possess similar “pepper pot” type structure, the spectral signatures exhibit enough characteristic differences to allow the unambiguous identification of conspecific individuals. By cross-correlating the position of the individuals of each species in the CIE chromaticity diagram with their flying period it was possible to show that relatively similarly looking, closely related species fly in distinct periods. The spectral identification method may prove useful in the investigation of museum exemplars which cannot be harmed. As the self-assembled, quasiordered, “pepper pot” type photonic nanoarchitectures of various colors seem to pose milder constraints on the production process as compared with perfect photonic crystals, such nanoarchitectures may find practical applications in a wide range from the textile industry to environmentally friendly colorants.

Introduction

Vision and color constitute a very important communication channel in the living world. Color is used for sexual communication,^{1a–c} for cryptic behavior,^{2a–c} or for warning potential predators,³ so that color is subjected to strong evolutionary pressure. It influences the survival and reproduction chances. In this way the genes of individuals possessing the “wrong” color have a lesser chance to be transmitted to the next generation.

Color may originate from the chemical,^{4a} physical,^{4b} or both, chemical and physical properties of matter. Although the separation into “chemical” and “physical” origins is not always unambiguous, it may be helpful to distinguish between colors arising from dyes and pigments, essentially based on the selective absorption of certain wavelength ranges of visible light by intramolecular processes and between the colors arising from photonic crystal (PhC) type structures. If the color of the PhC is in the visible range then the characteristic size of its building elements will be in the range from tens to hundreds of nanometres. This latter group of colors is often mentioned as “structural” color because it is generated by the (nano)structure of essentially transparent media.

The concept of PhC or photonic band gap (PBG) material was introduced 20 years ago by Yablonovitch^{5a} and John.^{5b} These nanoarchitectures are composites of two materials with different optical properties. Due to its characteristic structure and to the refractive index contrast, the photonic nanocomposite is able to interact selectively with the electromagnetic radiation^{4b} so that certain wavelength ranges cannot propagate in the PhC material and will be fully reflected. PBG materials are a slightly broader category than the strictly understood PhCs, as they may include materials with only moderate spatial ordering of the components.⁶ To summarize, PhCs and PBG materials are composite materials that gain new physical properties due to the combination of properties of the component materials and due to the particular nanostructure of the photonic nanocomposite. Both the alteration of the structure and of the materials building up the composite will change the optical properties (color).

Interestingly enough, the above mentioned photonic nanoarchitectures invented by mankind only 20 years ago were present on our planet since more than 500 million years.^{7a} Not only in the mineral world, as beautiful opals, but also widely spread in the living world from animals living deep in the sea^{7b} to butterflies and birds flying high in the sky.^{7c,d} While man made devices and components usually exploit a wide range of materials with often very different physical and chemical properties, the biological structures can be built using a much narrower range of materials, not to mention the very different processing conditions. Technology often uses intensive energy input in the process (“heat and beat”) to shape the material or alters the properties of a certain material. Biological building

^aResearch Institute for Technical Physics and Materials Science, PO Box 49, H-1525 Budapest, Hungary; Web: <http://www.nanotechnology.hu/>. E-mail: biro@mfa.kfki.hu; Fax: +36-1 392-2226

^bHungarian Natural History Museum, Baross utca 13, H-1088 Budapest, Hungary

processes take place in the vicinity of room temperature and under mild conditions, most frequently they are directed by self-assembly type processes. Most of the desired functionalities are achieved with materials constituted of: C, H, N, O, Ca, Mg atoms and a few trace elements. Instead of using a variety of materials and energy intensive processing, biology relies on structure and information.⁸ In particular, the very delicate wings and the wing scales of butterflies are nanocomposites of chitin and air. Chitin even with its refractive index of 1.56⁹ can provide enough refractive index contrast to generate a variety of structural colors—most frequently blues and greens are found in butterflies and beetles.

The often colorful wings of butterflies are covered by scales with typical dimensions in the range of $100 \times 50 \times 1 \mu\text{m}^3$. Extensive studies have been published on butterfly wing coloration, which is frequently attributable only to pigments,¹⁰ a topic not discussed in our work. The scales are built from chitin and they have the shape of a flattened sack. The side closer to the wing membrane (lower membrane) is usually unstructured, while the opposite side (upper membrane) most often has a complex micro- and nanostructure of ridges and cross-ribs linking the ridges, and other, more specialized elements. The flattened sack has a thin pedicel which fixes it in a flexible manner into the socket in the wing membrane. The system of scales is arranged in a regular way, like the tiles on a roof. The photonic nanoarchitectures responsible for color can be located in the volume of the scale—this is the case for the butterflies investigated in the present work. For a more detailed presentation of scale structure and color generation mechanisms see Ref. 11. The scales are formed during the pupation by self-assembly,¹² however, the exact mechanism is not known precisely.

In the past decade a continuous interest was manifested towards photonic nanoarchitectures occurring in butterflies and beetles, for a recent review of the most important results see Ref. 11 and references therein. The reason of this interest is to be found on one hand in the possibility of “copying” the colors, glossiness and metallic appearance which is often achieved for example by beetles and butterflies in an environmentally friendly way. Indeed, the insects in nature are part of sustainable ecosystems, which means that they are made from renewable materials that are broken down and recycled in a harmless way when the insect dies. In the same time, if kept in proper conditions, the colors can be preserved unaltered for several hundreds of years, as proven by museum collections.

All over the world, numerous natural history museums host impressive collections of butterflies and beetles. Fully along the principles of their duties, museum curators are extremely reluctant in sacrificing the museum specimens for invasive physical testing. On the other hand, for example, to carry out reproducible spectral measurements, the angle and distance of the illumination source and the conditions under which the reflected light are collected have to be under precise control. Usually, one has to detach the wings of butterflies and fix them on a rigid support to make sure that the above conditions are fulfilled. In order to overcome this contradiction, we developed a special instrument, the “spectroboard” inspired by the setting board used by entomologists, that will allow the reproducible measurement of large numbers of specimens without the need of harming them.

In the present paper we demonstrate the use of the spectroboard to investigate the quasicrystalline^{13a-c} “pepper pot” type¹⁴

photonic nanoarchitectures of nine Lycaenid butterfly species living in similar habitats with overlaps of their flying period. The dorsal side of the wings of male butterflies in the case of all investigated species has blue coloration of different hues. Entomologists distinguish these and other blue Lycaenid species on the basis of complex patterns occurring on the ventral sides of their wings. It is very unlikely that butterflies in flight may have enough “computing power” for mate/competitor recognition using these intricate patterns. On the other hand, the blue sexual signaling color of different hues may constitute a clear enough discriminating signal. The spectral signatures of the different blues, analyzed using an artificial neural network software, show that despite the fact that all examined species possess “pepper pot” type structure, the spectral signatures exhibit enough characteristic differences which allow the unambiguous identification of conspecific individuals.

Experimental

Materials

The present work is based on the examination of nine *Polymommatus* species (Fig. 1), in total 110 individuals. All the specimens were collected in the proximity of Budapest (Hungary) hills. All butterfly specimens originated from the curated Lepidoptera collection of the Hungarian Natural History Museum (HNHM), this made possible to have reliable information both on the location and time of the capture. The number of destroyed butterfly specimens was kept the minimum possible, all vouchers can be found in the HNHM.

Methods

Scanning electron microscope (SEM) investigations were done on pieces of wings $<1 \text{ cm}^2$ using LEO 1540 XB. To prevent parasitic charge effects, a previous gold sputtering was done and the wing pieces were mounted with a conductive carbon tape. For transmission electron microscope (TEM) (Tecnai) 80 nm thick layers were cut by ultramicrotome from pieces of wings embedded in special resin blocks.

Optical spectroscopy was carried out using Avantes 2048-2 modular fiber optic spectrometer in two setups. With the Avantes integrating sphere it is possible to collect light emerging under a wide angular range from the illuminated surface. In our case the sample (butterfly wing) is illuminated close to perpendicular, while the reflected light is collected in the whole upper hemisphere. This setup is useful for rough surfaces with highly angle dependent reflectivity to obtain within a single measurement light reflected under any angle. The main disadvantage of this method is in the sample preparation: the detachment of wing from the body is needed.

Due to the large number of individuals used in the study it was necessary to elaborate a measurement method that allowed the reproducible spectral characterization of the butterflies without harming the museum specimens. This method could prove useful for being used in general in museums as it does not harm the specimens, while it safely yields reproducible spectra. It is based on the wooden setting board used by the entomologists. We developed an instrument constituted from a basis reminiscent of the board with additional mechanical parts that allows the

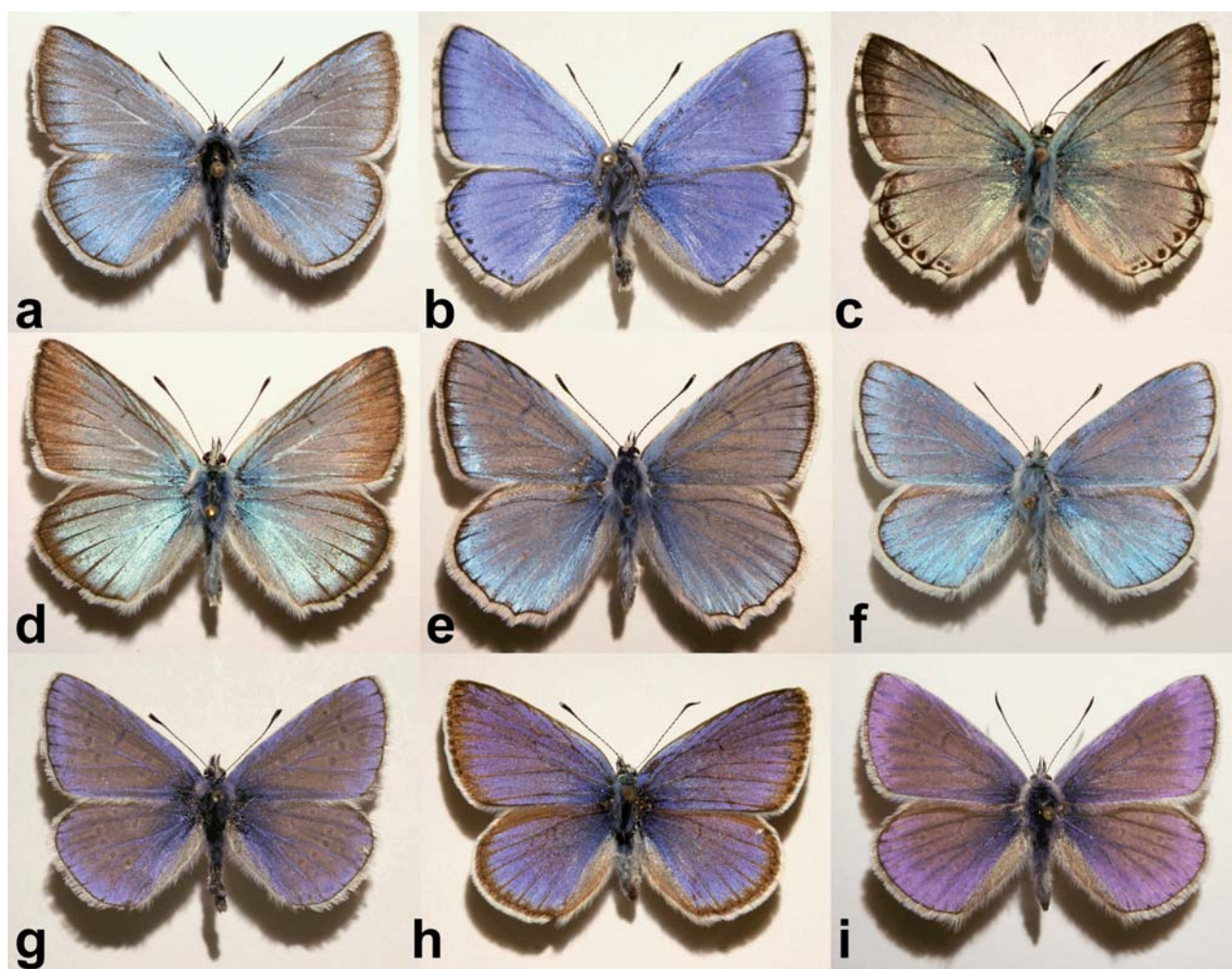


Fig. 1 Dorsal side perpendicular view photographs of the nine investigated *Polyommatus* species: (a) *P. amandus*, (b) *P. bellargus*, (c) *P. coridon*, (d) *P. damon*, (e) *P. daphnis*, (f) *P. dorylas*, (g) *P. icarus*, (h) *P. semiargus*, and (i) *P. thersites*. Mean wingspan is 3–3.5 cm. The shadow position indicates the light incidence angle.



Fig. 2 “Spectroboard” in use. Prepared specimens can be measured rapidly and safely in reproducible conditions. The Avantes fiber optic probe is set perpendicular to the wing surface. In the left upper side is placed the white, diffuse reference standard.

illuminator and pick-up fiber (Avantes reflection probe) to move over butterfly wings at a fixed distance (Fig. 2). For details see Ref. 15. The light incidence and detection are perpendicular to the wing. On the board is also placed the white, diffuse reference

at the same distance from the fiber probe as the wing samples. This setup offers reproducible and characteristic spectra while it does not necessitate physical destruction of the specimens. To prove this and to analyze the recorded spectra we used the free version of NeuroSolutions 5 (www.neurosolutions.com) artificial neural network (ANN) software. It was a point of high emphasis to use as little human intervention in the spectral evaluation as possible.

To illustrate the color differences for a human observer, the measured spectra were converted to x and y parameters through the CIE 1931 standard observer color matching functions, and represented in CIE xy chromaticity diagram. Such a scheme is not available now for butterflies, but it is well known that butterflies have an increased sensitivity and selectivity in the blue and even UV ranges as compared to humans.¹⁶

Results and discussion

First a detailed documentation of each specimen was carried out by taking photographs on both dorsal and ventral sides, and the collection date and place were recorded. As an example to the

various dorsal blue colorations see Fig. 1. The ventral side is decorated with a rather complex pattern,¹⁷ but is not under consideration in the present work. The wingspan varies between 3 and 3.5 cm. With the naked eye one can distinguish hues from violet to greenish-blue.

As already mentioned, the blue dorsal color is originated by the nanostructure of the wing scales. The “pepper-pot” nanoarchitecture acts as a photonic band gap composite, the wing color is determined by the physical dimensions, arrangement and refractive index contrast of the composite components. The wing is mainly constituted of chitin, the structural differences should be responsible for different hues. To get an insight into the structure, SEM and TEM investigations were done. An exemplar was sacrificed from each species and prepared as described previously. Typical surface (Fig. 3) and cross section (Fig. 4) images reveal complex nanoarchitectures constituted from perforated planes of chitin. The difference between the species is in the number of planes and the variation of perforation shape. Transmission electron microscope imaging is necessary to have an idea about the in-depth structure.

For spectral measurement with the “spectroboard” we placed the specimens in the slot formed for this (Fig. 2) with care to set their position. To register well comparable spectra, all specimens were measured in the same region of the right forewing. We collected spectral data in the 200–1100 nm range for 10 (or more) exemplars of each species. Provided that a good concordance of spectral shapes is obtained from conspecific exemplars, a characteristic spectrum might be derived by averaging the curves. The averaged curves for the investigated species (each normalized to the highest peak) are presented in Fig. 5. The differences are significant enough to discriminate them by their shape. One may remark by examining with the naked eye the spectra that the closely related species tend to have spectra with strong similarities in shape.

For an automated classification with artificial neural network, a feature extraction is needed for every single spectra measured on all exemplars. Raw data preprocessing was done with “Origin 8” software (www.originlab.com), containing the following steps:

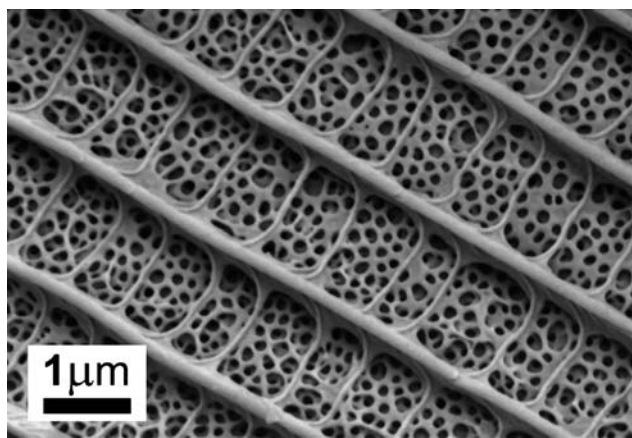


Fig. 3 Scanning electron micrograph of *Polyommatus thersites* dorsal scale. Between longitudinal ridges and cross-ribs linking these there is the pepper-pot structure.

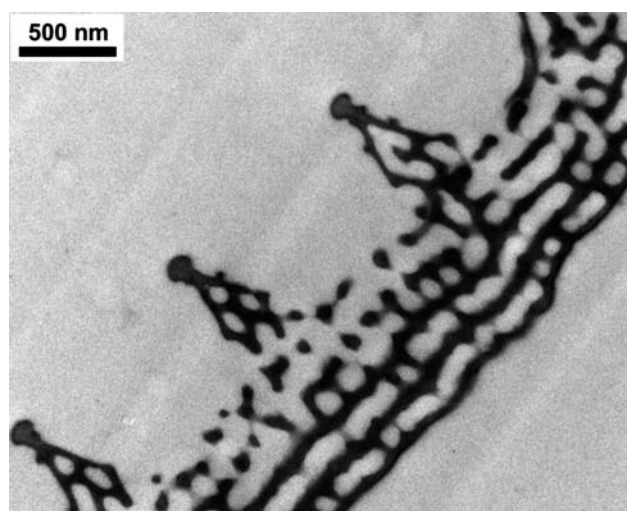


Fig. 4 Transmission electron microscope image of the *Polyommatus thersites* scale cross-section. From 5 parallel perforated chitin layers only the upper 2 are seen in SEM images. The ridges and the space under the ridges also contain nanostructures.

- crop to 220–800 nm range, to eliminate the noisy and irrelevant parts of the spectra
- high-frequency fluctuations were eliminated by FFT filtering
- normalizing to the highest peak
- background removal.

Next, using the “Origin 8” peak finding function for the present 2 (or 3, in some cases) peaks the following parameters were determined:

- the position of peak maximum in nm
- the intensity of the peak
- the position of base points on left and right side of peaks in nm
- the area of the peaks
- the peak full width at half maximum
- the left and right width of peak at half maximum (their ratio characterises the symmetry of the peak).

These parameters (8 for each peak, in total 16 or 24 for a species) describe the shape of curves with discrete values that are used as inputs for the ANN. For the three peak cases 18

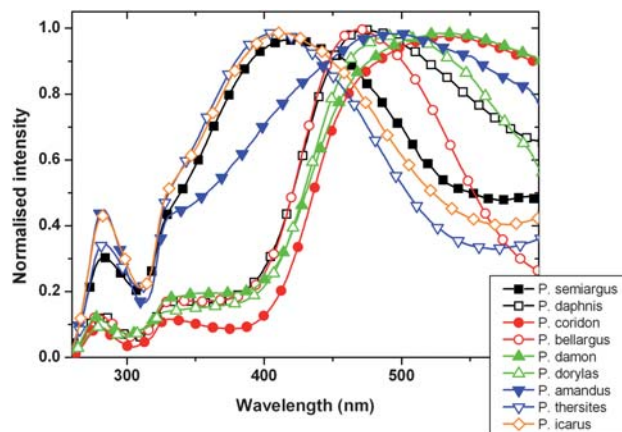


Fig. 5 Normalized average spectra of the nine *Polyommatus* species measured with the “spectroboard”.

Table 1 The artificial neural network identification results. Among the 55 tested exemplars only two were missed

Expected	<i>Daphnis</i>	<i>Coridon</i>	<i>Icarus</i>	<i>Thersites</i>	<i>Dorylas</i>	<i>Semiargus</i>	<i>Damon</i>	<i>Amandus</i>	<i>Bellargus</i>
Result									
<i>Daphnis</i>	5	0	0	0	0	0	0	0	0
<i>Coridon</i>	0	4	0	0	0	0	0	0	0
<i>Icarus</i>	0	0	5	1	0	0	0	0	0
<i>Thersites</i>	0	0	0	4	0	0	0	0	0
<i>Dorylas</i>	0	0	0	0	10	0	0	0	0
<i>Semiargus</i>	0	0	0	0	0	5	0	0	0
<i>Damon</i>	0	1	0	0	0	0	5	0	0
<i>Amandus</i>	0	0	0	0	0	0	0	5	0
<i>Bellargus</i>	0	0	0	0	0	0	0	0	10

relevant parameters were selected from the total of 24, in the two peak cases the parameters corresponding to the third, absent peak were set to zero. The network contains one hidden layer with 14 neurons, and 9 output neurons for the 9 species. Half of all of the specimens were used for the teaching process of the ANN with back propagation algorithm.¹⁸ After successful teaching, when the average squared error between the output and the target is small enough, the ANN was used on the remaining half of the exemplars to test the species recognition efficiency. The result (Table 1) presents the hit and misses as a table. From a number of 55 test exemplars 53 were identified correctly. One unsuccessful identification occurred in the case of *Polyommatus thersites* and *Polyommatus icarus*. Their spectral properties are very similar and they are closely related species. In the other misidentification a *Polyommatus damon* was the result instead of *Polyommatus coridon*. This may be attributed to the missing of blue scale in the case of *P. coridon* related with the age of the exemplar. The measured spectra contain more red if the ratio of blue cover scale and brownish ground scale number is smaller.

As a verification of the method, we carried out the neural network analysis on 30 spectra measured on 3 species (*Polyommatus coridon*, *P. thersites*, *P. dorylas*), 10 exemplars each. With the same processing and feature extraction a 100% accuracy was achieved. Our result with the “spectroboard” clearly shows

the possibility of efficient species determination by color measurement in a nondestructive way. This may be an important aspect in the case of the rare, valuable exemplars from museum collections and shows the power of this noninvasive, still reproducible measurement method.

Performing optical spectra analysis with artificial neural network we get a discrete result on specimens belonging to a species or not, but the amount of similarity is not quantified in a straightforward way. To demonstrate the variation of different blues, a graphic representation was done on data recorded with the “spectroboard”. Placing the *x* and *y* parameters of every spectrum on a CIE chromaticity diagram¹⁹ we get a densely populated cloud in the blue region. Zooming in and separating the species by oval lines for a clear view we get the graph on Fig. 6. One can notice that some species are overlapping while others are well separated by their color. If the butterflies are using color signals for mate recognition, simultaneous occurrence of specimens with identical color would be disturbing, and cause insecure continuation of the mating attempts.

To examine this hypothesis, data on the occurrence of the 9 species are needed. In the HNHM we noted the calendar day

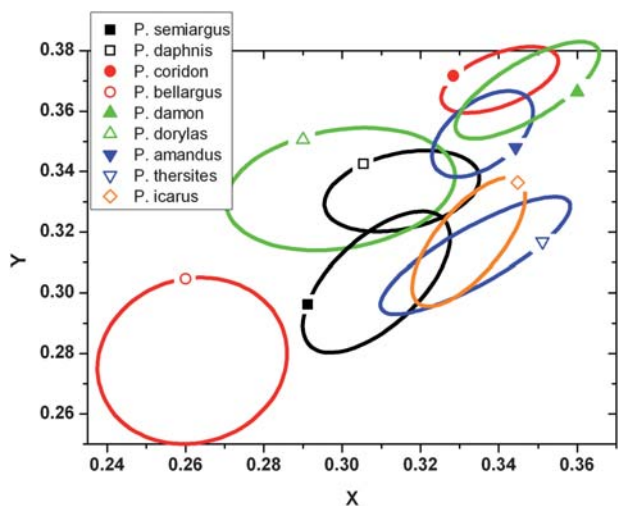


Fig. 6 Zoomed in CIE chromaticity diagram for the blue range. Inside the ovals are the *xy* plots for every specimen. Single plots are not marked for clarity.

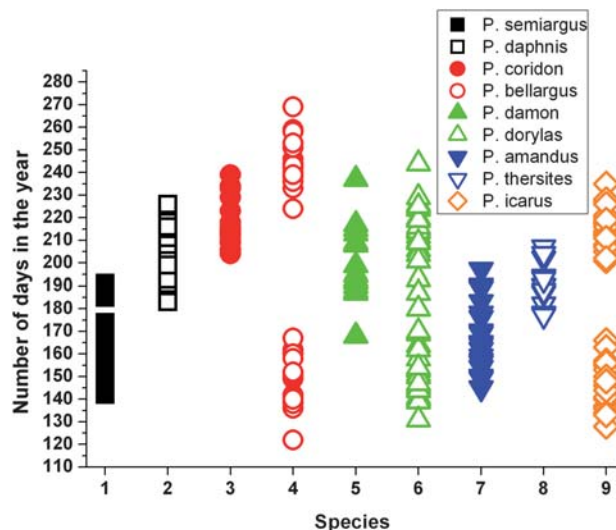


Fig. 7 Diagram representing temporal distribution of nine *Polyommatus* species. Note that *P. bellargus*, *P. dorylas* and *P. icarus* have two generations, in spring and in summer. Diagram made by randomly selecting museum specimens collected in the same habitat but in different years.

when the specimen was collected for exemplars from the same geographical region (Budapest hills). These data concerning the collection date define an interval for the occurrence. In Fig. 7 we represent the exemplars by species and days elapsed since 1st of January.

For instance the first appeared five species in spring *Polyommatus semiargus*, *Polyommatus bellargus*, *P. dorylas*, *Polyommatus amandus* and *P. icarus* are flying in the same period. Checking in the chromaticity diagram, their areas are well separated, meaning different hues for their dorsal coloration. From photographs (Fig. 1) one can also note the differences. In a reversed way, we can found overlapped areas on CIE diagram, for instance *P. icarus* and *P. thersites*. In the occurrence graph, *P. icarus* is shown in two separated generations while *P. thersites* fills up the gap between these two. In the end of *P. thersites* occurrence interval, the exemplars are old enough not to disturb the mating of *P. icarus*.

Conclusions

The self-assembled photonic nanoarchitectures of biologic origin occurring in the wing scales of the males of nine, blue colored Lycaenid butterflies were investigated by reflectance spectroscopy with a specially designed instrument which permitted the reproducible measurement of reflectance spectra without the need of destroying museum specimens. The measured spectra proved to be reproducible and to possess enough characteristics typical for a certain species to allow automated identification, with minimal human intervention. A neural network software was used after automated feature extraction by data processing software. The cross correlation of the regions occupied by the spectra of a certain species with the flying period of the species reveals that species with “similar” spectra fly in distinct periods.

The “spectroboard” and the data processing steps based on commercially available softwares were used successfully to identify numerous museum specimens on the basis of their spectra. This shows that spectral characterization can prove to be a useful tool in species identification without the need of harming the valuable specimens.

It was found that closely related species exhibit many similarities in their spectra but they can be discriminated. It is very likely that spectral measurements can be used as a fast and cheap way of checking the relationships of butterfly species in a group having common ancestry. It will be useful to compare the color based cladograms with cladograms established on the basis of other characteristics, regularly used by lepidopterists.

Last, but not least the variety of colors generated with the pepper pot type structures reveals the potential and the richness of these quasiordered, natural nanoarchitectures. It is obvious that the manufacturing of such quasiordered photonic nanoarchitectures poses far less constraints than the production of the perfectly ordered photonic crystals. Such quasiordered photonic nanoarchitectures may have numerous applications from the textile industry to traffic signs. It may constitute a major advantage that the color exhibited by these structures appears more intense with the increasing intensity of solar

illumination and the color perceived by an observer exhibits a significantly milder observation angle dependence as compared with the iridescent behavior of the perfect photonic crystals.

Acknowledgements

This work was supported by the Hungarian OTKA-NKTH-K grant 67793 and OTKA PD 83483. KK gratefully acknowledges financial support through the János Bolyai Research Scholarship of the Hungarian Academy of Sciences.

References

- (a) D. J. Kemp, *Proc. R. Soc. London, Ser. B*, 2007, **274**, 1043–1047; (b) D. J. Kemp, *Behav. Ecol.*, 2008, **19**, 1–9; (c) A. Loyau, D. Gomez, B. Moureau, M. Théry, N. S. Hart, M. Saint Jalme, A. T. D. Bennett and G. Sorci, *Behav. Ecol.*, 2007, **18**, 1123–1131.
- (a) S. Merilaita, J. Tuomi and V. Jormalainen, *Biol. J. Linn. Soc.*, 1999, **67**, 151–161; (b) K. Kertész, Zs. Bálint, Z. Vértésy, G. I. Márk, V. Lousse, J. P. Vigneron, M. Rassart and L. P. Biró, *Phys. Rev. E: Stat., Nonlinear, Soft Matter Phys.*, 2006, **74**, 021922–1–021922–15; (c) A. B. Bond and A. C. Kamil, *Nature*, 2002, **415**, 609–614.
- D. G. Ruxton, T. N. Sherratt, and M. P. Speed, *Avoiding Attack: the Evolutionary Ecology of Crypsis, Warning Signals and Mimicry*, Oxford University Press, 2004.
- (a) H. Zollinger, *Color Chemistry: Syntheses, Properties and Applications of Organic Dyes and Pigments*, Wiley, Weinheim, 3rd revised edn, 2003; (b) J. D. Joannopoulos, R. D. Meade, J. N. Winn, *Photonic Crystals: Molding the Flow of Light*, Princeton University Press, 1995.
- (a) E. Yablonovitch, *Phys. Rev. Lett.*, 1987, **58**, 2059–2062; (b) S. John, *Phys. Rev. Lett.*, 1987, **58**, 2486–2489.
- K. Edagawa, S. Kanoko and M. Notomi, *Phys. Rev. Lett.*, 2008, **100**, 013901–1–013901–4.
- (a) A. R. Parker, *Proc. R. Soc. London, Ser. B*, 1998, **265**, 967–972; (b) A. R. Parker, *J. Exp. Biol.*, 1998, **201**, 2343–2347; (c) M. Srinivasarao, *Chem. Rev.*, 1999, **99**, 1935–1962; (d) S. Kinoshita, *Structural Colors in the Realm of Nature*, World Scientific, New Jersey, 2008.
- J. F. V. Vincent, O. A. Bogatyreva, N. R. Bogatyrev, A. Bowyer and A.-K. Pahl, *J. R. Soc., Interface*, 2006, **3**, 471–482.
- P. Vukusic, J. R. Sambles, C. R. Lawrence and R. J. Wootton, *Proc. R. Soc. London, Ser. B*, 1999, **266**, 1403–1411.
- H. F. Nijhout, *The Development and Evolution of Butterfly Wing Patterns*, Smithsonian Institution Press, 1991.
- L. P. Biró and J. P. Vigneron, *Laser Photonics Rev.*, 2010, DOI: 10.1002/lpor.200900018.
- H. Ghiradella, *J. Morphol.*, 1989, **202**, 69–88.
- (a) L. P. Biró, K. Kertész, Z. Vértésy, G. I. Márk, Zs. Bálint, V. Lousse and J.-P. Vigneron, *Mater. Sci. Eng., C*, 2007, **27**, 941–946; (b) K. Kertész, G. Molnár, Z. Vértésy, A. A. Koós, Z. E. Horváth, G. I. Márk, L. Tapasztó, Zs. Bálint, I. Tamáska, O. Deparis, J. P. Vigneron and L. P. Biró, *Mater. Sci. Eng., B*, 2008, **149**, 259–265; (c) G. I. Márk, Z. Vértésy, K. Kertész, Zs. Bálint and L. P. Biró, *Phys. Rev. E: Stat., Nonlinear, Soft Matter Phys.*, 2009, **80**, 051903–1–051903–11.
- L. P. Biró, Zs. Bálint, K. Kertész, Z. Vértésy, G. I. Márk, Z. E. Horváth, J. Balázs, D. Méhn, I. Kiricsi, V. Lousse and J.-P. Vigneron, *Phys. Rev. E: Stat., Nonlinear, Soft Matter Phys.*, 2003, **67**, 021907–1–021907–7.
- Zs. Bálint, J. Wojtusiak, G. Piszter, K. Kertész and L. P. Biró, *Genus*, 2010, **21**, 163–168.
- A. D. Briscoe, *J. Exp. Biol.*, 2008, **211**, 1805–1813.
- E. A. Artem'eva, *Russ. J. Ecol.*, 2007, **38**, 58–67.
- R. Rojas, *Neural Networks—A Systematic Introduction*, Springer-Verlag, Berlin, New York, 1996.
- Y. Ohno, *Proceedings of IS&T NIP16 International Conference on Digital Printing Technologies*, Vancouver, 2000.